Renewable Energy 163 (2021) 2029–2036

Contents lists available at ScienceDirect

Renewable Energy

journal homepage: www.elsevier.com/locate/renene

Numerical simulation of the Mexico wind turbine using the actuator disk model along with the 3D correction of aerodynamic coefficients in OpenFOAM

Shayesteh Amini [a], Mahmood Reza Golzarian [a, *], Esmail Mahmoodi [b], Andres Jeromin [c], Mohammad Hossein Abbaspour-Fard [a]

[a] Department of Biosystems Engineering, Ferdowsi University of Mashhad, Mashhad, Iran
[b] Department of Biosystems Engineering, Shahrood University of Technology, Shahroud, Iran
[c] Department of Mechanical Engineering, Kiel University of Applied Sciences, Kiel, Germany

ARTICLE INFO

Article history:
Received 4 December 2019
Received in revised form
30 August 2020
Accepted 26 October 2020
Available online 29 October 2020

Keywords:
Actuator disk theory
BEM Theory
Numerical analysis
Wind turbine performance

ABSTRACT

A foremost element in aerodynamic behavior analysis of wind turbines is numerical simulation. Actuator disk model is a method which enables us to simulate and analyze the flow fields and wakes behind the rotor by reducing the fluid computation around the rotor and solving the Navier-Stokes equations without considering the blade boundary layer. In addition of the need for constructing a realistic geometrical model, one also must run a simulation with very small grid spacing and time steps to resolve the blade boundary layer dynamics leading to the aerodynamic forces, which is also extremely expensive. In this paper actuator disk model along with a 3D corrected aerodynamic coefficients was implemented in the OpenFOAM software to simulate the MEXICO wind turbine rotor. The simulations were performed under three conditions: turbulent, design and stall conditions. The results of simulation including an estimation of the blade forces and the wakes velocity field were compared with the experimental results. It was found that the 3D corrected aerodynamic coefficients of airfoils led to an improved agreement between the simulation and experimental results, compared to a model implementing original aerodynamic coefficients.

1. Introduction

Nowadays wind energy technology has well developed among all other renewable energy resources and is considered as a large-scale electricity generation resource. Low costs of wind-generated electricity has motivated many countries all over the world to manufacture small and large wind turbines as well as conducting extensive research on the optimization of wind-generated electricity generation [1]. Application of computational methods in wind turbine design started from the middle 19th century by using Integral Momentum theory and further developed gradually by analytical models like Blade Element Momentum (BEM) theory [26]. Computational fluid dynamics (CFD) has been successfully implemented with lower cost and less time than the experimental methods [2]. The first model to analyze a simple wind turbine was proposed by Betz et al., in 1926 which can be used for an ideal wind turbine power estimation. This simple model based on linear momentum theory. According to the Betz law no wind turbine can extract more than 59.3% of the wind kinetic energy. So, the maximum power coefficient of 0.593 is called Betz's limit [3].

With the development of computational techniques, CFD (computational fluid dynamics) method is widely used to perform research on predicting the aerodynamic performance of wind turbines [4]. Flow computation and analysis around a wind turbine rotor using common CFD methods that require boundary layer computation both on the blades and in the wakes are very costly. In recent years the most common and cost-effective methods for wind turbines rotors simulation has been using the actuator models, Actuator Disk Model (ADM), Actuator Surface Model (ASM) and Actuator Line Model (ALM), in which the blades are presented as a volume force defined on a disk or a surface or a node [5,28,29]. Compared to other models, the actuator disk model has a smaller mesh volume, a higher computation speed as well as an acceptable accuracy [2,6].

* Corresponding author. Department of Biosystems Engineering, Ferdowsi University of Mashhad, Azadi Square, Mashhad, 9177-948-978, Iran.
E-mail address: m.golzarian@um.ac.ir (M.R. Golzarian).

https://doi.org/10.1016/j.renene.2020.10.120
0960-1481/

Although the BEM theory is the only method widely used in the industrial design of wind turbine rotors, researchers have developed many advanced methods to predict the turbines performance. ADM uses BEM theory to calculate turbine forces within a porous disk: the method is formulated to compute blade lift and drag forces that are then averaged over annular elements, using information such as chord length, rotation rate, angle of attack, number of blades, tip and hub loss corrections, etc. The N–S or Euler equations are used to predict the velocities used in those calculations, and those forces can thus return thrust and torque forces to the flow as source terms to the governing equations. The actuator disk is a circular and permeable disk which is used instead of the turbine rotor. This permeable disk has a volume geometry equivalent to the rotor size. The center of volume elements contain a group of volume forces (force per unit volume: momentum forces). The calculated momentum forces can affect the Navier-Stokes equations in the fluid dynamics computations [7]. Many studies have been conducted using the actuator disk model, which are briefly reviewed in the following section.

The first non-linear actuator disc model for heavily loaded propellers was formulated by Wu [8]. The first implementation of the Actuator disk model was first presented by Ref. [9] for simulating the flow field around a fan in the OpenFOAM CFD solver. Then, Jeromin et al. developed the actuator disk model for the MEXICO rotor in the OpenFOAM solver and compared the results with a simple BEM, an actuator disk model in the FLUENT code and experimental data [10]. Mahmoodi et al. simulated a horizontal axis turbine (HAWT) using actuator disk model and modeled the flow field using Reynolds-averaged Navier–Stokes (RANS) and Laminar Navier-Stokes (LNS) turbulence models. They compared the results with the MEXICO experiment data which indicated that there was a good agreement between the LNS model on actuator disk with the experiments [11,12]. They simulated the wind tunnel and wind turbine completely and showed that the actuator disk can suitably simulate the Particle Image Velocimetry (PIV) results of the turbine wakes and also the exerted forces on the blades [13]. In addition to wind turbine simulation, the modified actuator disk model has been used to simulate the airplanes propellers and other machines that have a thrust generator which are similar to wind turbines [14–16].

Flow separation and stall phenomenon are very important in the aerodynamic behavior of wind turbine rotors. These phenomena are three dimensional and thus restrict the use of two dimensional airfoil data in the design and simulation processes. Therefore the aerodynamic coefficients need to be corrected [17]. Experience has revealed that points of wind turbine performance are greatly impacted by aerodynamic forces produced by wind [1]. The three-dimensional wind field has a severe influence on the wind turbine performance and the exerted loads on the blades. Considering the three-dimensional wind field on airfoils result in an increase of lift coefficient and thus a performance improvement of airfoils and blades. This is seen distinctively at higher wind speeds.

Reviewing the previous literature in wind turbine simulation shows that only a limited number of studies used correction coefficients and the 3D correction has not been used in the actuator disk model yet. Correction coefficients are presented by different equations. It is possible to assess the effect of each coefficient on the turbine performance and check if a particular coefficient improves the simulation in a specific software. This method is not exact and is error-prone so it is necessary to develop, implement and correct the model to obtain more realistic results. In this paper the MEXICO wind turbine is simulated, incorporating the actuator disk model along with the 3D correction of aerodynamic coefficients.

2. Numerical model

2.1. Governing equations

Since the air flow around a wind turbine is very slow in comparison with the speed of sound (lower than 0.3 Mach), the flow can be assumed incompressible along with steady-density assumption. Hence, it is possible to predict the flow characteristics by solving the 3D-incompressible Navier-Stokes equations. The incompressible Navier-Stokes equations are defined as:

$$\rho\left(\frac{\partial \vec{V}}{\partial t}+\vec{V}.\nabla\vec{V}\right)=-\nabla p+\nabla.\vec{\tau}+\vec{f} \tag{1}$$

where $\vec{V}$ is the velocity, t is the time. The density ρ is constant throughout the computational domain, p the pressure, $\nabla.\vec{\tau}$ is volumetric forces due to fluid viscosity, $\vec{f}$ represents external volume forces such as gravity, centrifugal force and any other external forces acting on the fluid element.

The mass continuity equation is also needed to predict the fluid movement. Assuming incompressible (steady-density) flow, the mass continuity equation is:

$$\vec{\nabla}.\vec{V}=0 \tag{2}$$

2.2. Actuator disk model and calculation of the exerted forces

In the modified actuator disk model, the rotor is replaced by a physical permeable disk in Navier-Stokes equations. It includes a permeable disc with complete planar or spatial geometry the size of rotor. It is possible to add a group of unit forces (unit force per area or volume: momentum forces) to the center of its planar or spatial components. So, one of the disk inner elements in a particular distance from the center of rotation is chosen and the moments are exerted on it. Since the Navier-Stokes equations are in Cartesian coordinate system, the coordinate of the element's center is (x, y, z) and its velocity components are $\vec{V}=(V_x, V_y, V_z)$. Through the rest of this paper, cylindrical coordinate system is used because of the cylindrical shape of the disk in the model and the relationship of the blade aerodynamic properties with tangential direction.

Fig. 1 shows the velocity and force vectors of the airfoil section, the airfoil inlet velocity and flow angle are:

$$w=\sqrt{V_\theta^2+V_z^2}=\sqrt{(r\Omega+V_{\theta,w})^2+V_z^2} \tag{3}$$

$$\phi=\tan^{-1}\left(\frac{V_z}{r\Omega+V_{\theta,w}}\right) \tag{4}$$

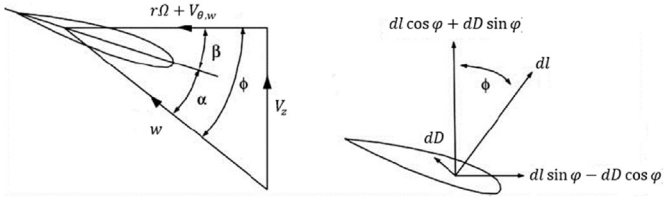

Fig. 1. The velocity and force vectors formulation to calculate the moments of the modified actuator disk.

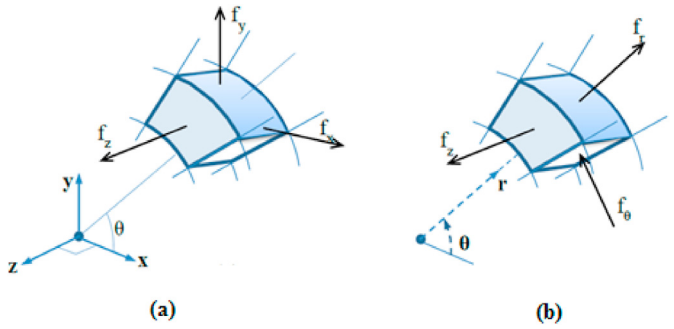

Fig. 2. (a) The force components of the fluid element are in Cartesian coordinate during the measurement. (b) The conversion of fluid element Cartesian components to polar components using their position measurement in the computations.

Having the flow angle and importing global pitch angle and twist angle, the angle of attack is:

$$\alpha = (\phi - \gamma) = [\phi - (\beta + \delta)] \tag{5}$$

Having the angle of attack, the airfoil lift and drag coefficients at that point are obtained from the experimental values. Therefor it is possible to calculate the differential values of lift and drag forces by the following equations:

$$dL = \frac{1}{2}\rho W^2 c C_l \tag{6}$$

$$dD = \frac{1}{2}\rho W^2 c C_d \tag{7}$$

The fluid element is then rotated around the rotor axis to produce an annular element in the disk whose front area is $2\pi r t_h$, in which t_h is the disk thickness (0.2 m). Thus the axial and tangential forces as illustrated in Fig. 2 -which are per annular element volume-could be calculated as:

$$f_\theta = \frac{\rho}{2t_h} W^2 \sigma' (C_l \sin\phi - C_d \cos\phi) \tag{8}$$

$$f_z = \frac{\rho}{2t_h} W^2 \sigma' (C_l \cos\phi + C_d \sin\phi) \tag{9}$$

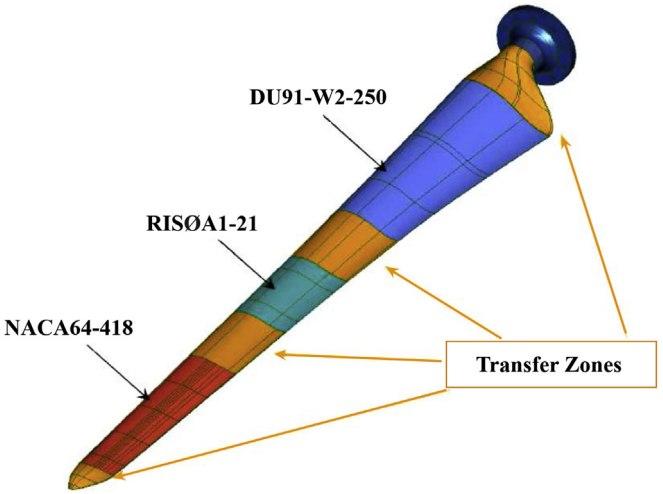

Fig. 3. The rotor blade designed by the blade design team [19].

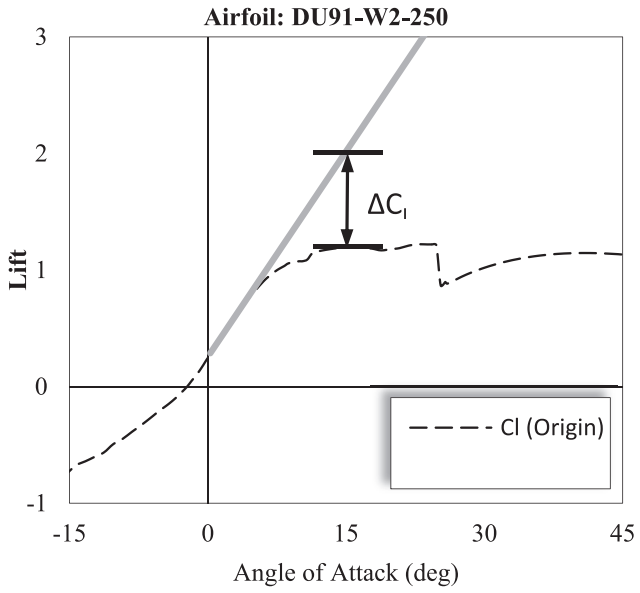

Fig. 4. The preparation of lift coefficients for 3D conversion [12].

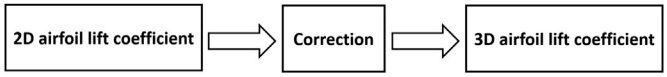

Fig. 5. Three-dimensional correction algorithm.

where σ' is calculated from $Bc/2\pi r$, B indicates the number of blades and c is the blade chord length.

Since the Navier-Stokes computations are performed in the Cartesian coordinate system, regarding Fig. 2, the volume forces calculated from Equations (8) and (9) are converted from cylindrical to Cartesian coordinate, so:

$$f_x = \frac{\rho}{2t_h} W^2 \sigma' (C_l \sin\phi - C_d \cos\phi)\sin\theta \tag{10}$$

$$f_y = \frac{\rho}{2t_h} W^2 \sigma' (C_l \sin\phi - C_d \cos\phi)\cos\theta \tag{11}$$

$$f_z = \frac{\rho}{2t_h} W^2 \sigma' (C_l \cos\phi + C_d \sin\phi) \tag{12}$$

As previously described, when fluid is passing through the fluid element, the exerted forces on the fluid element could be calculated

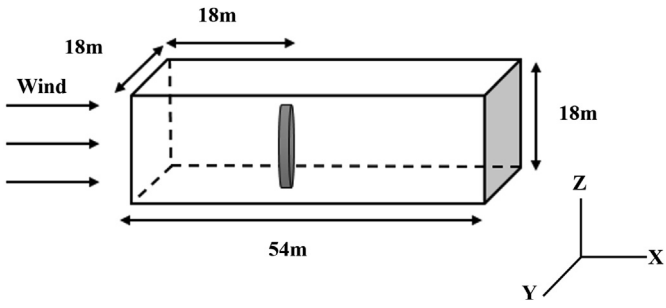

Fig. 6. Computation domain and the position of turbine within it.

using the above-mentioned equations and the data of airfoil characteristics. These volume forces are written as $\overrightarrow{f} = (f_x, f_y, f_z)$. Afterward, this vector volume force is transferred to the fluid element center and takes the place of the external force, $\overrightarrow{f}$ of the Navier-Stokes equation in the fluid elements.

In this research, Spalart-Allmaras model applied within the RANS scheme, was used to model the wakes around the rotor and the turbulent flow resulting from rotating blades. Spalart-Allmaras (SA) is a turbulence model used for modeling different type of turbulent flows, specifically aerodynamic flows. The S-A is a one-equation turbulence model and formed with the transport equation of the kinematic eddy viscosity $\tilde{\nu}$. This equation is written by:

$$\frac{\partial(\rho\tilde{\nu})}{\partial t} + div(\rho\tilde{\nu}U_i) = \frac{1}{\sigma_\nu} div[(\mu + \rho\tilde{\nu})\nabla\tilde{\nu}] + \rho C_{b1}\tilde{\nu}\tilde{\Omega} - \rho C_{w1}\left(\frac{\tilde{\nu}}{ky}\right)f_w \tag{13}$$

where

$$\tilde{\Omega} = \Omega_{ij} + \frac{\tilde{\nu}}{(ky)^2} f_{v2} \tag{14}$$

and $\tilde{\nu}$is the kinematic eddy viscosity, $\tilde{\Omega}$is the local mean vorticity, $\Omega_{ij}$is the mean vorticity tensor, the function $f_{v2} = f_{v2}\left(\tilde{\nu}/\nu\right)$and $f_w$are the further wall damping functions, $\mu$is the dynamics viscosity, y is the distance to the solid wall. The constants include σ_ν, C_{b1}, $C_{b2}$and k have value of 0.67, 0.1355, 0.622 and 0.4187, respectively [18].

3. Experimental baseline and modelling approach

3.1. Mexico experiments

The MEXICO (Model Experiment in Controlled Conditions) project was funded by the European Union in 2006 to enable various institutes and universities perform their research activities. The Energy Research Center of Netherland (ECN) as the manager of the MEXICO project established an integrated research group called MexNext by contracting some well-known universities in order to develop different theories in wind turbine modelling. The MEXICO experiment was carried out on a 4.5 m diameter, Three-blade wind turbine in the DNW/LLF wind tunnel. The test cross section of the wind tunnel is variable which can produce the maximum speed of 55 m/s (corresponding to 3.9×10^7 Reynolds number) by a 9.5 m × 9.5 m test section whereas a range of 0.01–0.42 Mach is covered by its smallest test section. The blades of this turbine were formed by 3 airfoils including DU91-W2-250, RISØ A1-21 and NACA64-418 along with transfer zones between them (Fig. 3). To measure pressure distribution, 148 pressure sensors were installed in 5 sections on the blades. In the MEXICO project three sets of experiments were conducted on the wind turbine: three wind

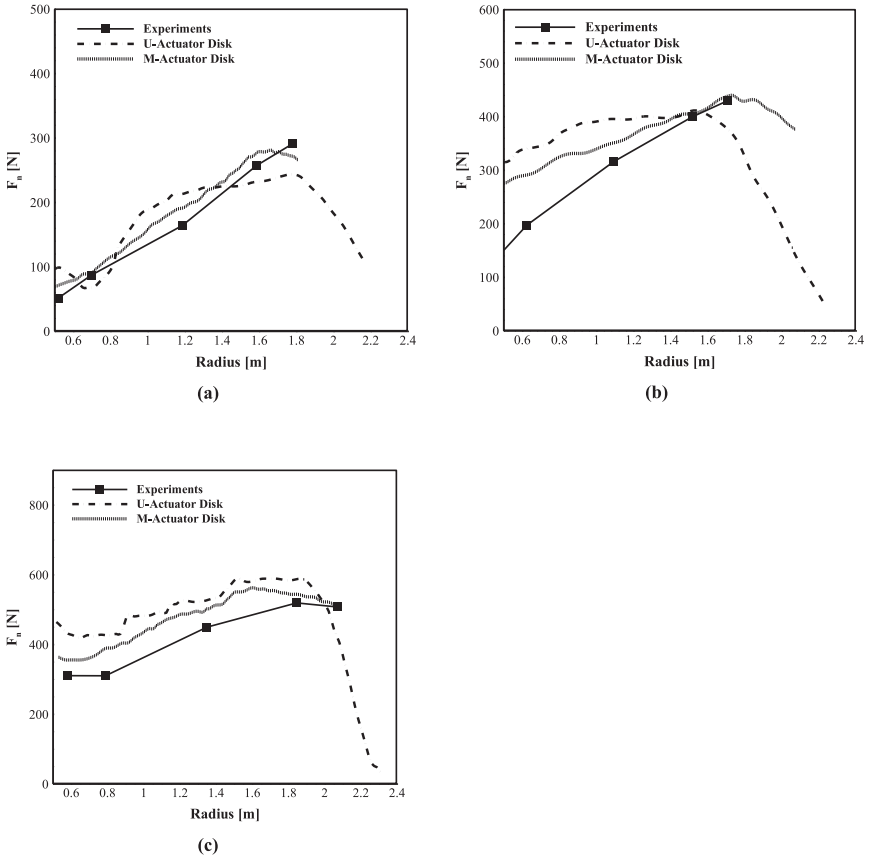

Fig. 7. The axial force distribution along the blade length (Experiments [13], Unmodified Actuator Disk, Modified Actuator Disk): (a) in the turbulence region (10 m/s wind speed) and (b) in the design region (15 m/s wind speed) and (c) in the stall region (24 m/s wind speed).

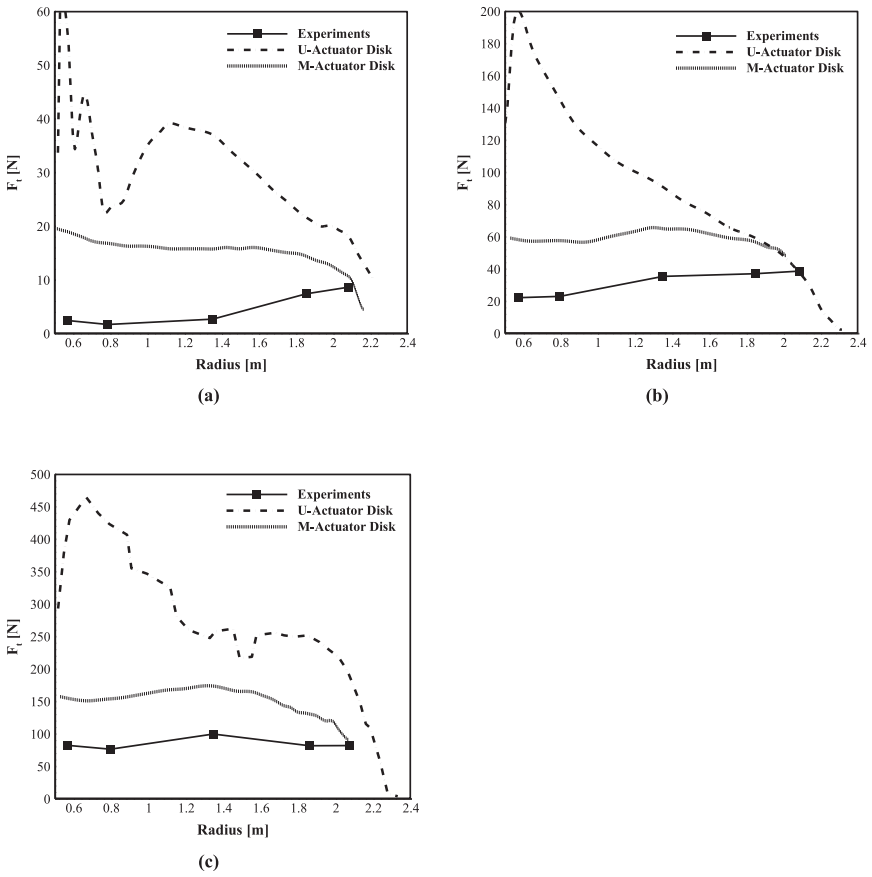

Fig. 8. The tangential force distribution along the blade length (Experiments [13], Unmodified Actuator Disk, Modified Actuator Disk): (a) in the turbulence region (10 m/s wind speed) and (b) in the design region (15 m/s wind speed) and (c) in the stall region (24 m/s wind speed).

speeds of 10, 15 and 25 m/s defined as turbulence, design and stall conditions, respectively. In the first set, velocity field of the upper and lower parts of the rotor disk were measured. In the second set, the upstream and downstream velocity field were measured. Finally, the third set of experiments were done to detect and track the vorticities around and near the turbine [19,20].

3.2. Turbine modelling and computational setup

The 2D airfoil data comprise of the lift and drag coefficients were provided from experiments. Since measuring 3D data is expensive, researchers use different methods to correct 2D to 3D airfoil data ([21–24]. In 1993, Snel proposed his theory for data correction of the lift coefficient as:

$$C_{l,\,3D} = C_{l,\,2D} + J\left(\frac{c}{r}\right)^{H}\left(C_{l,\,inv} - C_{l,\,2D}\right) \tag{15}$$

where J and H are constant coefficients which varies between 2 to 3 and 1 to 2, respectively; c is the cord, and r is the radial distance from the rotation center. Considering the previous literature, the values of 3 and 2 were selected for J and H, respectively (snel, 1993). $C_{l,\,inv}$ is the lift coefficient when the fluid is considered completely inviscid. From a mathematical point of view, it is derived from the extension of tangent line of lift curve in low angles of attack. $\Delta C_l = C_{l,\,inv} - C_{l,\,2D}$ is the difference between two curves (Fig. 4). Hence using this Equation (15), it is possible to convert the 2D lift data (i.e. $C_{l,\,2D}$) to 3D data (i.e. $C_{l,\,3D}$)[12] (see Fig. 5).

In this paper, the governing equations were solved by the OpenFOAM open-source software, by implementing and adding the actuator disk model along with 3D corrected aerodynamic coefficients to its library in three steps: a) implementing correction, b) calculating baseline with the basic model and c) calculating with additional 3D corrections on lift and drag. In order to analyze the effect of 3D corrected aerodynamic coefficients on the modified actuator disk theory, at first the model was solved without this correction for the turbulence, design and stall conditions (the wind speed of 10, 15 and 24 m/s, respectively). Afterward, the function of the 3D corrected lift coefficients were applied to the actuator disk model and solved again for the three aforementioned speeds.

In this paper, the PISO algorithm was used for determining velocity-pressure correlation. Spalart-Allmaras model is applied within the RANS scheme, was used to model the wakes around the rotor and the turbulent flow resulting from rotating blades. In this software, numerical finite volume method is used for numerical solution of partial differential equations.

3.3. Computational domain

The computations of this study are based on a Cartesian coordinate system. The main fluid flow direction follows the x-axis, the z-axis describes the height." That y-axis is the width follows

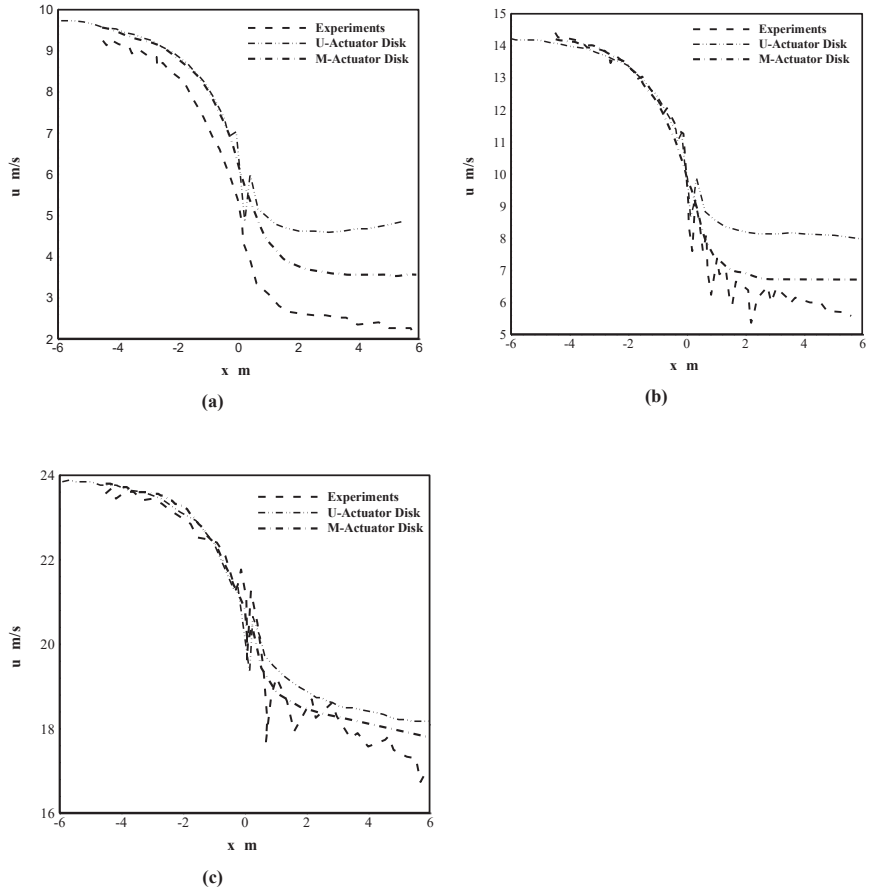

Fig. 9. The distribution of the axial component of the wake velocity in the flow longitudinal direction (Experiments [13], Unmodified Actuator Disk, Modified Actuator Disk): (a) in the turbulence region (10 m/s wind speed) and (b) in the design region (15 m/s wind speed) and (c) in the stall region (24 m/s wind speed).

automatically by choosing a Cartesian coordinate system. The computation domain is a $54 \times 18 \times 18$ m^3 cube (Fig. 6). The turbine rotor is placed within a distance 4 times the diameter, 18 m, from the inlet and is completely aligned in center from sides. The mesh was generated using a block rectangular mesh with structured grid spacing in each direction.

The boundary conditions for speed and pressure field are given as:

Initial value for the pressure is zero. The boundary condition for the mean inlet pressure, the zero gradient condition and for the mean outlet pressure, the condition of atmospheric pressure is considered. Initial value for the velocity is V_0. It means calling the main values of the input speed (in this work, 10, 15 and 24 m/s). The boundary condition for the velocity is similar to the pressure.

4. Simulation results

The simulation results are reported in two sections: the axial and tangential forces distribution and wakes velocity field. For the validation of simulation results, the MEXICO rotor (with stall-regulated blade) experimental data in turbulence, design and stall conditions at speeds of 10, 15 and 24 m/s, the constant rotational speed of 424 rpm, the tip speed ratio of 10, 6.7 and 4.2 and constant pitch angle of -2.3° in the free flow were used [19].

4.1. Resolved axial and tangential forces

In Figs. 7 and 8, the axial and tangential forces are shown along the radius of the rotor for each of the three wind speed conditions for the experiments, the unmodified actuator disk and the modified actuator disk. The axial forces of the modified actuator disk (Fig. 7) are closer to the experimental data than the unmodified actuator disk. Especially for the low wind speed (high tip speed ratio) there can be seen a drop in the force predicted by the unmodified actuator disk in the transition area from DU91-W2-250 to RISØ A1-21 profile (0.6 r 0.8). This drop is because of weakness of the UAD model in the transition area. This was corrected by the modified actuator disk model The impact of 3D corrections is much greater for the tangential forces in Fig. 8. The computed forces are still not perfect but much closer to the experimental data.

4.2. Wakes velocity field results

In this section, the wakes prediction results are reported and validated in axial and tangential directions. To study the wakes, the data were collected from two sensors which were installed in the flow longitudinal direction and the blade radial direction. The longitudinal sensor was placed in the 61% blade radius ($r = 1.37m$) and was used to record data in the induction and wake regions. The radial sensor was placed at a distance of 0.3 m after the rotor and was used to record data [20,25].

In Figs. 9 and 10 show the distribution of the axial component of the wake velocity in the longitudinal direction and the radial direction of flow for each of the three wind speed conditions for the experiments, the unmodified actuator disk and the modified actuator disk, respectively. The data were collected from the radial PIV data monitoring at 0.3 m distance through the turbine downstream.

In Fig. 9, the axial component of wake velocity distribution (Downstream) was overestimated. Both implemented models could predict a behavior pattern similar to the experiments. Using the 3D correction model resulted in a more accurate wake behavior prediction. As seen in the actual velocity change (experiments) in these graphs, there was a remarkable decrease in the axial velocity after the rotor disk ($x = 0$) and wake velocity fluctuations in this region. These fluctuations were likely caused by the conversion of the blades cross section geometry from DU91-W2-250 airfoil to RISØ A1-21 airfoil. Since the RISØ A1-21 airfoil had different aerodynamic coefficients of lift force compared with the other airfoils, it led to some changes in the strength of vorticities around this region and caused fluctuations.

According to Fig. (10a) both models could cover most of the turbulence region data and predict the similar wake behavior pattern. According to Fig. 10, within a distance approximately 54% blade radius ($r = 1.2$ m), a considerable decrease in the experimentally measured velocity is seen. This phenomenon might be due to vorticity release from the tip of the blades in the transition area between DU91-W2-250 and RISØ A1-21 airfoils which caused errors in measuring and recording data by PIV system. According to these figures, there was a good agreement between the models and experiments in the near tip regions.

5. Conclusion

In this paper the wakes behind the MEXICO experiment turbine were simulated and the exerted forces on the blades were predicted using actuator disk model along with 3D correction of aerodynamic coefficient and RANS turbulence model in the OpenFOAM software. The simulation were performed for three conditions: turbulence (10 m/s wind speed), design (15 m/s wind speed) and stall (24 m/s wind speed). The simulation results were validated by the experimental data. Ignoring a few exceptions, there were good agreements between the simulation results and the experimental data. According to the 2D aerodynamic characteristics of the blade airfoils, the measurement conditions and characteristics of RISØ airfoil are different from the others. The lift coefficients in the stall region were different. At 10° angle of attack, there was a large disparity between predicted forces and experimental data for RISØ A1-21 section of the blade. Therefore the data of this airfoil, which is located in the middle of the blade, is different from the other two airfoils in the unmodified model. Thus a jump in the force distribution results were expected in this part of the blade. Since the airfoil aerodynamic data is 2D, it does not match with the

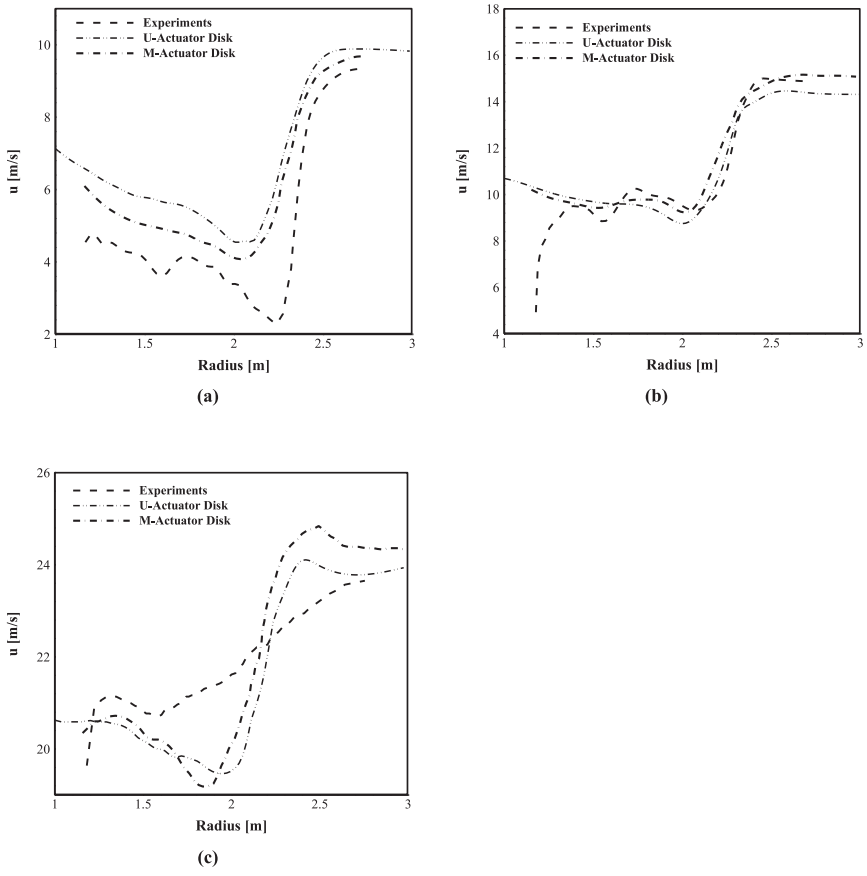

Fig. 10. The axial component distribution of wake velocity in the blade radial direction (Experiments [13], Unmodified Actuator Disk, Modified Actuator Disk): (a) in the turbulence region (10 m/s wind speed) and (b) in the design region (15 m/s wind speed) and (c) in the stall region (24 m/s wind speed).

experiments in unmodified actuator disk mode. The unmodified actuator disk predicts incorrect behavior from loads on the blade, especially tangential forces in the area close to the center of rotation because it uses 2D coefficients. The modified actuator disk converts 2D lift coefficients to 3D lift coefficients. It is considering the flow effects in the radial direction that delays the stall phenomenon in high speeds. In this paper, the flow effects in the radial direction was the main purpose of using 3D correction in the actuator disk model. The effect of radial flows on the airfoil results in an increase of lift coefficient and thus a performance improvement of airfoils and blades that, it is not possible to be assessed in the airfoils 2D experiments. The use of modified coefficients in the stall state of rotor improves the amount of computational error, significantly.

CRediT authorship contribution statement

Shayesteh Amini: Investigation, Software, Visualization, Writing - original draft. **Mahmood Reza Golzarian:** Conceptualization, Methodology, Supervision, Visualization, Project administration, Writing - review & editing. **Esmail Mahmoodi:** Conceptualization, Methodology, Supervision, Visualization, Writing - review & editing. **Andres Jeromin:** Validation, Writing - review & editing. **Mohammad Hossein Abbaspour-Fard:** Writing - review & editing.

Declaration of competing interest

The authors declare that they have no known competing financial interests or personal relationships that could have appeared to influence the work reported in this paper.

Acknowledgment

The authors acknowledge the support the Ferdowsi University of Mashhad, Iran (grant no. 37498).

References

[1] M. Bilgili, A. Yasar, Performance evaluation of a horizontal axis wind turbine in operation, Int. J. Green Energy 14 (12) (2017) 1048–1056, https://doi.org/10.1080/15435075.2017.1357039.
[2] T. Kim, S. Oh, K. Yee, Improved actuator surface method for wind turbine application, Renew. Energy 76 (2015) 16–26.
[3] J.F. Manwell, J.G. McGowan, A.L. Rogers, Wind Energy Explained: Theory, Design and Application, second ed., John Wiley & Sons, 2011 https://doi.org/10.1002/9781119994367. Print ISBN: 978047001500. Online ISBN: 9781119994367.
[4] H. Yang, W. Shen, H. Xu, Z. Hong, C. Liu, Prediction of the wind turbine performance by using BEM with airfoil data extracted from CFD, Renew. Energy 70 (2014) 107–115.
[5] J.N. Sørensen, W.Z. Shen, Numerical modeling of wind turbine wakes, J. Fluid Eng. 124 (2) (2002) 393–399, https://doi.org/10.1115/1.1471361.
[6] F. Castellani, A. Vignaroli, An application of the actuator disc model for wind turbine wakes calculations, Appl. Energy 101 (2013) (2013) 432–440.
[7] R. Mikkelsen, Actuator Disc Methods Applied to Wind Turbines. PhD Thesis, Department of Mechanical Engineering. Technical University of Denmark, Denmark, 2004.
[8] J.N. Sørensen, A. Myken, Unsteady actuator disc model for horizontal axis wind turbines, J. Wind Eng. Ind. Aerod. 39 (Issues 1–3) (1992) 139–149, 1992.
[9] E. Svenning, Implementation of an Actuator Disk in Open FOAM. Developed for Open FOAM-1.5-dev, 2010.
[10] A. Jeromin, A. Bentamy, A.P. Schaffarczyk, Actuator disk modeling of the Mexico rotor with Open FOAM, in: Paper Presented at the First Symposium on OpenFOAM® in Wind Energy, ITM Web of Conferences, vol. 2, 2014, 06001, https://doi.org/10.1051/itmconf/20140206001. February 18.
[11] E. Mahmoodi, A.P. Schaffarczyk, Incompressible Navier-Stokes against RANS turbulent model for wake modeling via actuator disc theory, in: EAWE 4th Conference: the Science of Making Torque from Wind Conference, 2012. Oldenburg, Germany.
[12] E. Mahmoodi, A. Jafari, A.P. Schaffarczyk, A. Keyhani, J. Mahmoudi, A new correlation on the Mexico experiment using a 3D enhanced blade element momentum technique, Int. J. Sustain. Energy 33 (2) (2014) 448–460, https://doi.org/10.1080/14786451.2012.759575.
[13] E. Mahmoodi, A. Jafari, A. Keyhani, Wind turbine rotor simulation via CFD based actuator disc technique compared to detailed measurement, Int. J. Renew. Energy Dev. 4 (3) (2015) 205–210, https://doi.org/10.14710/ijred.4.3.205-210.
[14] F.L. Chuiton, Actuator disc modelling for helicopter rotors, Aero. Sci. Technol. 8 (4) (2004) 285–297, https://doi.org/10.1016/j.ast.2003.10.004.
[15] P. Beaumier, J.M. Bousquet, Appliyed CFD for Analysing Aerodynamic Flows Around Helicopters, 24th International Congress of the Aeronautical Sciences, ICAS, Châtillon, France, 2004.
[16] P. Reynier, U. Reisch, J.M. Longo, R. Radespiel, Flow predictions around a missile with lattice wings using the actuator disc concept, Aero. Sci. Technol. 8 (5) (2004) 377–388, https://doi.org/10.1016/j.ast.2004.03.003.
[17] I. Herráez, B. Stoevesandt, J. Peinke, Insight into rotational effects on a wind turbine blade using Navier–Stokes computations, Energies 7 (10) (2014) 6798–6822, https://doi.org/10.3390/en7106798.
[18] C. Suvanjumrat, Comparison of turbulence models for flow past NACA0015 airfoil using OpenFOAM, Eng. J. 21 (3) (2017) 207–221.
[19] H. Snel, J.G. Schepers, B. Montgomerie, The Mexico project (Model Experiments in Controlled Conditions): the database and first results of data processing and interpretation, in: Journal of Physics: Conference Series vol. 75, IOP Publishing, 2007, 012014, https://doi.org/10.1088/1742-6596/75/1/012014, 1.
[20] K. Boorsma, J.G. Schepers, Description of Experimental Setup MEXICO Measurement, ECN-X–11-120, ECN, Netherlands, 2011.
[21] H. Snel, R. Houwink, G.J. VanBussel, A. Bruining, Sectional prediction of 3D effects for stalled flow on rotating blades and comparison with measurements, Eur. Comm. Wind Energy Conference. H.S. Stephens & Assoc, Travemunde, Lubeck, Germany (1993) 395–399.
[22] Z. Du, M.S. Selig, A 3-D stall-delay model for horizontal axis wind turbine performance prediction, AIAA paper, 21, https://doi.org/10.2514/6.1998-21, 1998.
[23] P.K. Chaviaropoulos, M.O. Hansen, Investigating three-dimensional and rotational effects on wind turbine blades by means of a quasi-3D Navier-Stokes solver, J. Fluid Eng. 122 (2) (2000) 330–336, https://doi.org/10.1115/1.483261.
[24] C. Bak, Sensitivity of key parameters in aerodynamic wind turbine rotor design on power and energy performance, J. Phys. Conf. 75 (1) (2007), 012008, https://doi.org/10.1088/1742-6596/75/1/012008. IOP Publishing.
[25] K. Boorsma, J.G. Schepers, Description of Experimental Setup MEXICO Measurement, ECN, Netherlands, 2009.
[26] H. Glauert, Airplane propellers, in: Aerodynamic Theory, Springer Berlin Heidelberg, 1935, pp. 169–360.
[28] W.Z. Shen, J.N. Sørensen, J.H. Zhang, Actuator surface model for wind turbine flow computations, Proceedings of the EWEC (2007).
[29] N. Troldborg, J.N. Sørensen, R.F. Mikkelsen, Actuator Line Modeling of Wind Turbine Wakes. PhD Thesis, Technical University of Denmark, 2008.